Redundant Regulation of Cdk1 Tyrosine Dephosphorylation in *Saccharomyces cerevisiae*

Erin K. Kennedy,* Michael Dysart,* Noel Lianga,* Elizabeth C. Williams,* Sophie Pilon,* Carole Doré,*,† Jean-Sebastien Deneault,* and Adam D. Rudner*,1

*Ottawa Institute of Systems Biology and Department of Biochemistry, Microbiology and Immunology, University of Ottawa, ON K1H 8M5, Canada, and †Ottawa Hospital Research Institute, The Ottawa Hospital, ON K1H 8L6, Canada

ORCID ID: 0000-0002-0301-1042 (A.D.R.)

ABSTRACT Cdk1 activity drives both mitotic entry and the metaphase-to-anaphase transition in all eukaryotes. The kinase Wee1 and the phosphatase Cdc25 regulate the mitotic activity of Cdk1 by the reversible phosphorylation of a conserved tyrosine residue. Mutation of *cdc25* in *Schizosaccharomyces pombe* blocks Cdk1 dephosphorylation and causes cell cycle arrest. In contrast, deletion of *MIH1*, the *cdc25* homolog in *Saccharomyces cerevisiae*, is viable. Although Cdk1-Y19 phosphorylation is elevated during mitosis in *mih1*Δ cells, Cdk1 is dephosphorylated as cells progress into G_1, suggesting that additional phosphatases regulate Cdk1 dephosphorylation. Here we show that the phosphatase Ptp1 also regulates Cdk1 dephosphorylation *in vivo* and can directly dephosphorylate Cdk1 *in vitro*. Using a novel *in vivo* phosphatase assay, we also show that PP2A bound to Rts1, the budding yeast B56-regulatory subunit, regulates dephosphorylation of Cdk1 independently of a function regulating Swe1, Mih1, or Ptp1, suggesting that $PP2A^{Rts1}$ either directly dephosphorylates Cdk1-Y19 or regulates an unidentified phosphatase.

KEYWORDS Cdc25/Mih1; Cdk1; PP2A; Wee1/Swe1; mitosis

MITOTIC onset is regulated in all eukaryotes by an increase in Cdk1 activity caused by the dephosphorylation of Cdk1 on a conserved inhibitory tyrosine (tyrosine 19 in budding yeast) (Nurse 1990). The Wee1 kinase phosphorylates and inhibits Cdk1 (Gould and Nurse 1989; Parker *et al.* 1992), and the Cdc25 phosphatase acts as a mitotic inducer by dephosphorylating and activating Cdk1 (Dunphy and Kumagai 1991; Gautier *et al.* 1991). *wee1* mutants in fission yeast shorten G_2 by prematurely activating Cdk1 (Nurse 1975; Russell and Nurse 1987), whereas *cdc25* mutants cannot accumulate sufficient Cdk1 activity to enter mitosis and arrest (Russell and Nurse 1986). Both Wee1 and Cdc25 are the targets of numerous cell-cycle checkpoints, all of which delay mitotic entry by activating Wee1 or inhibiting Cdc25 (Kellogg 2003). In budding yeast, Swe1 (the Wee1 homolog) and Mih1 (the Cdc25 homolog) also function prior to mitosis (Russell *et al.* 1989; Booher *et al.* 1993; Harvey and Kellogg 2003; Pal *et al.* 2008), but our recent work revealed that overexpression of Swe1 or activation of a Swe1-dependent checkpoint arrests cells in metaphase (Lianga *et al.* 2013).

Deletion of *cdc25* in fission yeast is lethal and arrests cells in G_2, indicating the essential role of Cdk1-Y15 dephosphorylation in fission yeast (Russell and Nurse 1986). In contrast, although deletion of *MIH1* exhibits high Cdk1-Y19 phosphorylation during mitosis, these cells have only mild delays in mitotic entry and anaphase onset and initiate Cdk1-Y19 dephosphorylation at anaphase onset (Russell *et al.* 1989; Rudner *et al.* 2000; Pal *et al.* 2008; Lianga *et al.* 2013). This behavior argues that at least one additional phosphatase functions redundantly with Mih1.

Russell and colleagues (Millar *et al.* 1992) identified the fission yeast Pyp3 as a phosphatase that functions redundantly with Cdc25. Increased expression of *pyp3* or the budding yeast and mammalian homologs *PTP1*, PTP1B and TC-PTP1, respectively, suppresses the temperature sensitivity of *cdc25-22*, and the *pyp3*Δ mutant exacerbates the defects of *cdc25-22* (Gould *et al.* 1990; Millar *et al.* 1992; Hannig *et al.* 1993), suggesting that Ptp1 has a conserved function dephosphorylating Cdk1.

doi: 10.1534/genetics.115.182469
Manuscript received September 28, 2015; accepted for publication December 21, 2015; published Early Online December 29, 2015.
Supporting information is available online at www.genetics.org/lookup/suppl/doi:10.1534/genetics.115.182469/-/DC1
[1]Corresponding author: Department of Biochemistry, Microbiology and Immunology, University of Ottawa, 451 Smyth Rd., RGN 4501J, Ottawa, ON K1H 8M5, Canada. E-mail: arudner@uottawa.ca

Protein phosphatase 2A (PP2A) also may act redundantly with Mih1. PP2A is a heterotrimeric complex composed of a catalytic subunit, a scaffolding subunit, and one of two B-regulatory subunits, Cdc55 (homologous to B55/B) or Rts1 (homologous to B56/B′) (Healy *et al.* 1991; Stark 1996; Shu *et al.* 1997; Zhao *et al.* 1997). Deletion of *CDC55* or *RTS1* elevates Cdk1-Y19 phosphorylation (Minshull *et al.* 1996; Zapata *et al.* 2014), and both mutants display synthetic interactions when combined with *mih1*Δ (Pal *et al.* 2008; Costanzo *et al.* 2010), suggesting that PP2A may function with Mih1. However, these synthetic interactions instead may be explained by negative regulation of Swe1 by $PP2A^{Cdc55}$ and $PP2A^{Rts1}$ (Harvey *et al.* 2011). In addition, although PP2A is capable of tyrosine dephosphorylation *in vitro*, it is believed to function solely as a serine/threonine phosphatase *in vivo* (Foulkes *et al.* 1983; Janssens and Goris 2001; Shi 2009; Tonks 2013).

Here we show that Ptp1, the budding yeast homolog of fission yeast Pyp3, also regulates Cdk1 dephosphorylation *in vivo*. However, despite delayed Cdk1-Y19 dephosphorylation in anaphase, *mih1*Δ *ptp1*Δ cells are as healthy as *mih1*Δ cells, suggesting the existence of an additional redundant phosphatase. Using an *in vivo* Cdk1-Y19 phosphatase assay, we show that $PP2A^{Rts1}$, but not $PP2A^{Cdc55}$, regulates dephosphorylation of Cdk1-Y19 independently of its role regulating Swe1. Although we are not able to confirm whether $PP2A^{Rts1}$ directly dephosphorylates Cdk1-Y19 or regulates an unidentified phosphatase, our results suggest that Mih1, Ptp1, and $PP2A^{Rts1}$ function redundantly to regulate the spatial and temporal activation of Cdk1, providing a mechanism for the observed stepwise activation of Cdk1 prior to anaphase onset.

Materials and Methods

A complete description of our methods can be found in Supporting Information, File S1.

Results

Ptp1 regulates Cdk1 tyrosine dephosphorylation

In fission yeast, the Pyp3 phosphatase acts redundantly with Cdc25 *in vivo* and *in vitro* (Millar *et al.* 1992), so we examined the role of the budding yeast homolog Ptp1 in regulating tyrosine phosphorylation on Cdk1. Asynchronously growing *ptp1*Δ cells have elevated Cdk1-Y19 phosphorylation (Figure 1A), but this increase is not as dramatic as what is observed in *mih1*Δ cells. (See Table S1 and Table S2 for a complete list of all the strains used in this study.)

*mih1*Δ *ptp1*Δ double mutants are viable and healthy, so we examined the effect of mutating both phosphatases on entry into and progression through mitosis. Deletion of *MIH1* causes an increase in Cdk1-Y19 phosphorylation during mitosis, delays mitotic entry, and the length of mitosis increases (Lianga *et al.* 2013) (Figure 1B). *ptp1*Δ mutant cells behave similarly to wild-type cells, but in *mih1*Δ *ptp1*Δ double-mutant cells, Cdk1-Y19 levels remain high as the cells progress through mitosis and reenter G_1. Surprisingly, despite this persistent phosphorylation, we observed no change in the timing of degradation of the mitotic cyclins Clb2 and Clb5, the anaphase inhibitor Pds1/securin, and the cohesin subunit Mcd1/Scc1 in *mih1*Δ *ptp1*Δ cells compared to *mih1*Δ cells. Although Cdk1-Y19 phosphorylation does not appear to drop as *mih1*Δ *ptp1*Δ cells exit mitosis, the lower levels present after G_1 arrest caused by the mating pheromone α-factor (αf; $t = 0$) suggest that an additional phosphatase may function redundantly with Mih1 and Ptp1.

Although the level of Cdk1-Y19 phosphorylation in *mih1*Δ and *mih1*Δ *ptp1*Δ cells is high relative to wild-type cells, it is lower than the extent of phosphorylation in wild-type cells arrested by the actin-depolymerizing drug latrunculin A (latA), which activates a Swe1-dependent checkpoint, or in cells overexpressing Swe1 (*GAL-SWE1*) (Figure 1C). These two treatments arrest the cell cycle and depend on Y19 phosphorylation on Cdk1 (Booher *et al.* 1993; Lew and Reed 1995), suggesting that small differences in Cdk1-Y19 phosphorylation have large phenotypic effects.

We assessed the extent of inhibition of Cdk1 activity caused by Y19 phosphorylation *in vivo* by measuring the Clb2-associated histone H1 kinase activity in synchronous mitotic cells (Figure 1D). By normalizing the activity to the total Cdk1 present in each kinase reaction, we were able to compare the relative activity and Y19 phosphorylation of each Cdk1/Clb2 complex present in a cell. Cdk1 precipitated from synchronous mitotic *mih1*Δ and *mih1*Δ *ptp1*Δ cells ($t = 75$ min after release from G_1 arrest) has approximately 65% of wild-type activity, while arrest caused by latA or *GAL-SWE1* further reduces Cdk1 activity to 50% of wild type. The reduction in Cdk1 activity in these cells is mirrored by concomitant increases in Cdk1-Y19 phosphorylation. These measurements also allow us to infer the relative stoichiometry of Cdk1-Y19 phosphorylation and suggest that small decreases in Cdk1 activity (and increased Y19 phosphorylation) in latA- or *GAL-SWE1*-arrested cells halts cell-cycle progression. These data are consistent with our prior observation that ∼30% of the Cdk1 remains active during an arrest caused by *GAL-SWE1* (Lianga *et al.* 2013).

Cdk1 precipitated from mitotic *swe1*Δ cells ($t = 60$ min) has threefold higher activity than Cdk1 from synchronous mitotic wild-type cells ($t = 60$ min) (Figure 1D), suggesting that two-thirds of the Cdk1 in mitotic wild-type cells is phosphorylated on Y19. We were surprised, however, that mitotic Cdk1 activity in wild-type cells does not differ from the activity of Cdk1 precipitated from wild-type or *swe1*Δ cells arrested in mitosis by nocodazole despite the lack of Cdk1-Y19 phosphorylation. We hypothesize that an unidentified mechanism reduces Cdk1 activity in nocodazole-arrested cells and may be used to control the increase in total Cdk1 activity as Clb2 protein rises during the arrest.

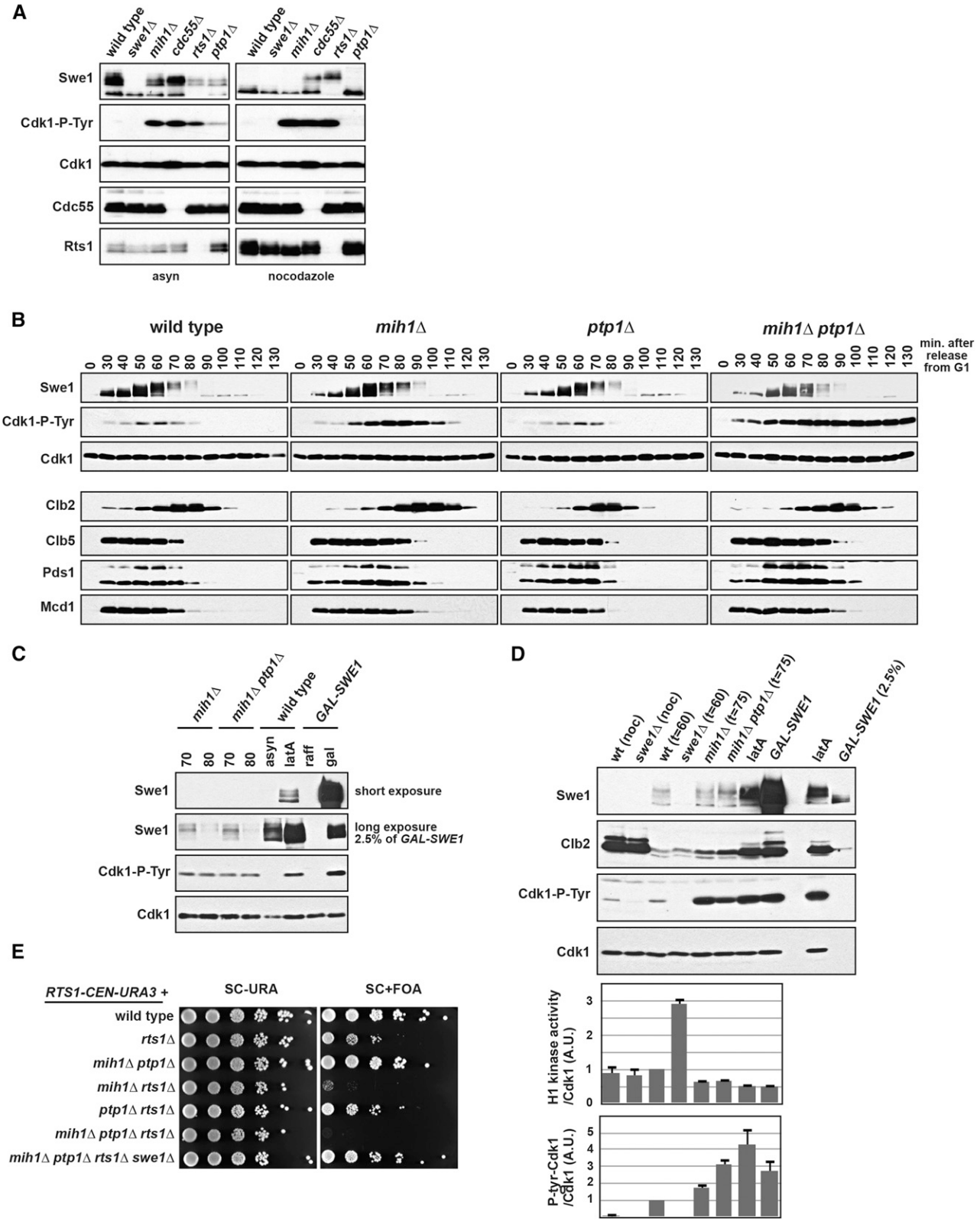

Figure 1 *PTP1* regulates Cdk1-Y19 phosphorylation *in vivo*. (A) *mih1*Δ, *cdc55*Δ, *rts1*Δ, and *ptp1*Δ cells have increased Cdk1-Y19 phosphorylation. Wild-type, *swe1*Δ, *mih1*Δ, *cdc55*Δ, *rts1*Δ, and *ptp1*Δ cells were grown at 25° asynchronously (asyn) or arrested in mitosis with nocodazole, harvested, lysed, and blotted with the indicated antibodies. (B) Wild-type, *mih1*Δ, *ptp1*Δ, and *mih1*Δ *ptp1*Δ cells were grown at 25°, arrested with mating pheromone, and released into the cell cycle at $t = 0$. Cells were harvested, lysed, and blotted with the indicated antibodies. (C) A comparison of Cdk1-Y19 phosphorylation in *mih1*Δ and *mih1*Δ *ptp1*Δ cells in samples from B at $t = 70$ min and $t = 80$ min, wild-type cells treated with latA (2.5 μM), and

PP2A^{Rts1} acts redundantly with Mih1 and Ptp1

Mutation of the B-regulatory subunits of PP2A, *CDC55* and *RTS1*, also causes an increase in Cdk1-Y19 phosphorylation (Minshull *et al.* 1996; Zapata *et al.* 2014) (Figure 1A). *cdc55*Δ and *rts1*Δ are also synthetically lethal or result in sickness, respectively, in combination with *mih1*Δ, and these interactions are completely suppressed by deletion of *SWE1* (Pal *et al.* 2008; Costanzo *et al.* 2010) (Figure 1E). In addition, the temperature sensitivity of *rts1*Δ is partially suppressed by *swe1*Δ (Figure S1A). The increase in Cdk1-Y19 phosphorylation in these mutants and their interaction with *mih1*Δ can at least be partially attributed to upregulation of Swe1 protein in both *cdc55*Δ and *rts1*Δ cells (Minshull *et al.* 1996; Harvey *et al.* 2011; Zapata *et al.* 2014) and downregulation of Mih1 in *cdc55*Δ cells (Pal *et al.* 2008), but it also may be caused by other functions of PP2A.

To test whether PP2A regulates Cdk1-Y19 phosphorylation independently of its function regulating Swe1 and Mih1, we developed an *in vivo* phosphatase assay in which we monitor Cdk1-Y19 dephosphorylation in mitotically arrested cells that first induce high levels of Swe1 and Cdk1-Y19 phosphorylation using galactose induction of a *GAL-SWE1-AID* gene, then rapidly repress *SWE1* transcription with glucose, and degrade the Swe1-AID protein with the addition of auxin (Figure 2). This experimental design allows us to assess the role of PP2A independently of its function regulating Swe1 and in the absence of Swe1-dependent rephosphorylation of Cdk1. *GAL-SWE1-AID* replaces the endogenous *SWE1*, so when grown on glucose, these strains behave effectively as *swe1*Δ cells, suppressing the lethality of several of the mutant combinations tested.

In *mih1*Δ cells, Cdk1 is dephosphorylated between 2 and 4 hr after the addition of glucose and auxin (Figure 2, A and B). If only glucose, but not auxin, is added, Swe1-AID is degraded slowly, and Cdk1-Y19 phosphorylation persists throughout the experiment. Cdk1 is dephosphorylated slowly in *mih1*Δ *ptp1*Δ cells (Figure 2A), consistent with our observation that these cells are defective in the dephosphorylation of Cdk1-Y19 in anaphase (Figure 1B). To simplify our analysis of these experiments, we added αf during the release from nocodazole, arresting cells in the subsequent G_1. We noticed that although adding either 25 ng/ml or 1 μg/ml of αf will arrest cells in G_1 (Figure S2, A and B), Cdk1-Y19 dephosphorylation in *mih1*Δ *ptp1*Δ cells is similar to that in *mih1*Δ cells when treated with a higher concentration of αf (Figure 2B). However, the triple-mutant combination *mih1*Δ *ptp1*Δ *rts1*Δ completely blocks dephosphorylation of Cdk1 at both concentrations of pheromone (Figure 2, A and B), suggesting that PP2A^{Rts1} may directly target Cdk1-Y19 or may negatively regulate an unidentified fourth phosphatase that targets Cdk1. Consistent with redundancy among these three phosphatases, the deletion of *PTP1* in *mih1*Δ *rts1*Δ cells causes lethality that is fully suppressed by deletion of *SWE1* (Figure 1E). Although *mih1*Δ *ptp1*Δ *rts1*Δ cells block Cdk1-Y19 dephosphorylation, they do not remain arrested in mitosis, as judged by the degradation of Clb2, Clb5, Pds1, and Mcd1 (Figure S2, A and B).

To investigate whether PP2A^{Cdc55} also functions independently of Swe1 to regulate Cdk1-Y19 dephosphorylation, we used strains containing *CDC55-AID* rather than a deletion of *CDC55* because *cdc55*Δ cells grow poorly in medium containing raffinose or galactose, both of which are used in this experiment (Figure S1B). In the presence of auxin, *CDC55-AID* is lethal in combination with *mih1*Δ, and strains containing *CDC55-AID* grow poorly on raffinose and galactose medium (Figure S1, B and C), suggesting that *CDC55-AID* behaves as a null mutant when such cells are grown on auxin. In the *in vivo* phosphatase assay, *mih1*Δ *CDC55-AID* and *mih1*Δ *ptp1*Δ *CDC55-AID* cells induce lower levels of Swe1-AID, but enough is produced to allow the accumulation of high levels of Cdk1-Y19 phosphorylation (Figure 2A). As in *mih1*Δ cells, Cdk1 is dephosphorylated between 2 and 4 hr after the addition of glucose and auxin, suggesting that PP2A^{Cdc55} regulates Cdk1-Y19 phosphorylation indirectly through Swe1 and Mih1. We were surprised that *mih1*Δ *ptp1*Δ *CDC55-AID* cells dephosphorylate Cdk1-Y19 more rapidly than *mih1*Δ *ptp1*Δ cells, suggesting that PP2A^{Cdc55} may have an additional function negatively regulating Cdk1-Y19 dephosphorylation.

Ptp1 dephosphorylates Cdk1 in vitro

To validate our genetic results, we tested whether purified phosphatases can dephosphorylate Cdk1 *in vitro* (Figure S3). Immunopurified Swe1-phosphorylated Cdk1/Clb2 complexes were incubated with Mih1, Ptp1, PP2A^{Cdc55}, or PP2A^{Rts1}

cells overexpressing Swe1 from a *GAL-SWE1* gene that replaces the endogenous *SWE1*. Cells arrested by latA or Swe1 overexpression have significantly more Swe1 than *mih1*Δ and *mih1*Δ *ptp1*Δ cells and have slightly higher levels of phosphorylated Cdk1-Y19. (D) Differences in Cdk1-Y19 phosphorylation correlate with changes in Cdk1/Clb2 histone ^{1}H-kinase activity. Wild-type, *swe1*Δ, *mih1*Δ, and *mih1*Δ *ptp1*Δ cells were grown in nocodazole (noc) or arrested with mating pheromone (αf; 100 ng/ml) and released into the cell cycle at *t* = 0 and either harvested at the time of peak Cdk1-Y19 phosphorylation (*t* = 60 or 75 min post-release) or incubated with latA for 2 hr. *GAL-SWE1* cells were grown in YEP + 2% raffinose, arrested in nocodazole, and then grown for 90 min after the addition of 2% galactose. Cells were harvested, lysed, and blotted with the indicated antibodies (top panels), or Cdk1/Clb2 complexes were immunoprecipitated with anti-Clb2 antibody and blotted with anti-Cdk1 and anti-Cdk1-P-tyr antibodies, or the Clb2-associated histone H1 kinase activity was assayed. The indicated ratios [average (±SEM) of three independent experiments] were calculated and normalized so that the ratio of synchronous mitotic wild-type cells (*t* = 60 min) is set to 1. (E) *mih1*Δ *rts1*Δ and *mih1*Δ *ptp1*Δ *rts1*Δ cells are inviable, and this inviablity is rescued by *swe1*Δ. Tenfold serial dilutions of the indicated strains were spotted on SC-URA or SC + FOA medium and grown at 25°. All strains harbor a *RTS1-CEN-URA3* plasmid, and their dependence on *RTS1* was examined by selecting for loss of the plasmid using 5-FOA, which counterselects for *URA3* cells.

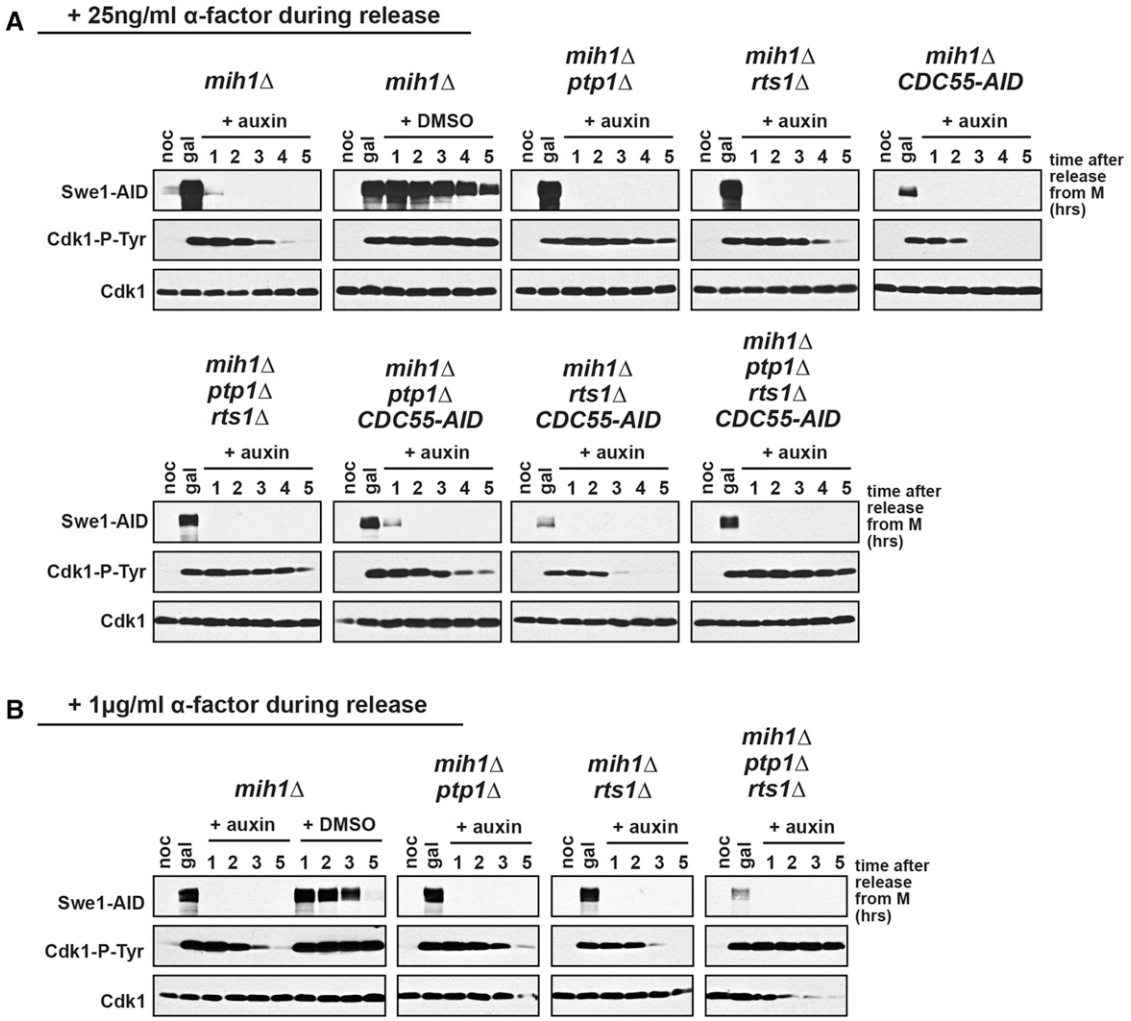

Figure 2 *MIH1*, *PTP1*, and *RTS1* redundantly regulate Cdk1-Y19 dephosphorylation. The indicated strains were grown overnight in YEP + raffinose at 25° and arrested in mitosis with nocodazole (noc), and then galactose was added to induce high levels of Swe1-AID and Cdk1-Y19 phosphorylation. After 1 hr of induction (gal), cells were released from the nocodazole arrest, dextrose was added to repress transcription of *GAL-SWE1-AID*, and auxin was added to induce Tir1-dependent degradation of Swe1-AID and Cdc55-AID, if present in the strain. Control *mih1*Δ cells also were released into medium containing dextrose and vehicle (DMSO). α-factor was added 90 min after release at (A) 25 ng/ml or (B) 1 μg/ml in order to rearrest the cells in the subsequent G_1. Cells were harvested at the indicated times for immunoblotting with the indicated antibodies.

purified from yeast, or with lambda phosphatase. Both Mih1 and Ptp1 can dephosphorylate Cdk1 *in vitro*, but both forms of PP2A and lambda phosphatase cannot (Figure 3). The dephosphorylation of a fortuitous background protein (indicated by an asterisk) confirms that purified $PP2A^{Cdc55}$ and lambda phosphatase are active in this experiment and that Mih1 and Ptp1, which do not dephosphorylate this protein, display Cdk1-Y19 specificity. $PP2A^{Rts1}$, which our prior experiments suggested may directly dephosphorylate Cdk1, had no activity in this experiment, but we have no evidence that the purified enzyme is active.

Discussion

We have identified two phosphatases, Ptp1 and $PP2A^{Rts1}$, that work redundantly with Mih1 to regulate Cdk1-Y19 dephosphorylation. Past work had suggested that Ptp1 may regulate Cdk1-Y19 dephosphorylation in budding yeast (Hannig *et al.* 1993), and we have shown that combining deletions in *PTP1* and *MIH1* severely impairs Cdk1-Y19 dephosphorylation during anaphase. *mih1*Δ *ptp1*Δ cells still dephosphorylate Cdk1-Y19 during a prolonged G_1 arrest, suggesting that at least one additional phosphatase may regulate Cdk1-Y19 dephosphorylation.

Cdk1-Y19 dephosphorylation in *mih1*Δ *ptp1*Δ cells could be caused by turnover of Cdk1 because newly synthesized Cdk1 would not be rephosphorylated by Swe1, which is absent in G_1 (Figure 1B). Although we did not directly measure the half-life of Cdk1 in budding yeast, we think this mechanism is unlikely or plays only a minor function because the half-life of Cdk1 in cultured mammalian cells in G_1 is ~18 hr (Welch and Wang 1992; Gannon *et al.* 1998).

To test whether PP2A functions redundantly with Mih1 and Ptp1, we developed a novel *in vivo* phosphatase assay

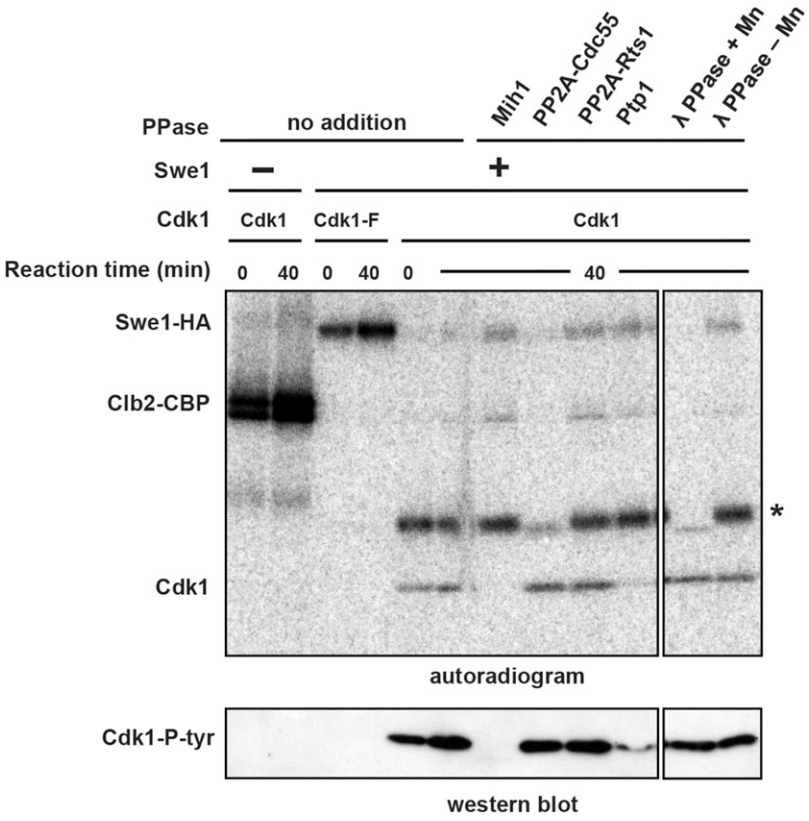

Figure 3 Mih1 and Ptp1 dephosphorylate Cdk1-Y19 *in vitro*. Purified Cdk1/Clb2-CBP was phosphorylated by bead-bound Swe1-HA in the presence of γ-[^{32}P]ATP. Following phosphorylation, Cdk1/Clb2-CBP was removed from the beads and mixed with purified phosphatases and an excess of unlabeled ATP to prevent rephosphorylation of Cdk1 by γ-[^{32}P]ATP and Swe1-HA that was washed off the beads. Reactions were run on a polyacrylamide gel and either dried and exposed to a phosphorimager screen or transferred to nitrocellulose and immunoblotted with anti-Cdk1-P-Y19 antibody. In the absence of Swe1-HA, Clb2 is heavily phosphorylated by Cdk1. In the presence of Swe1-HA, Clb2 is not phosphorylated, showing that Cdk1 is completely inhibited by Swe1-dependent phosphorylation of Y19. Swe1 does not phosphorylate Cdk1-F, but Cdk1-F phosphorylates Swe1 (Harvey *et al.* 2005). After incubation for 40 min at 25°, purified Mih1 and Ptp1 (see Figure S3) can dephosphorylate Cdk1-Y19 *in vitro*, but PP2A^{Cdc55}, PP2A^{Rts1}, and lambda phosphatase (λ-PPase) cannot. PP2A^{Cdc55} and λ-PPase can effectively dephosphorylate a fortuitous phosphorylated background protein (indicated with an asterisk), providing a control indicating that both PP2A^{Cdc55} and λ-PPase are active.

that allowed us to examine whether PP2A regulates Cdk1-Y19 phosphorylation independently of its known role regulating Swe1 and Mih1. We discovered that PP2A^{Rts1} either directly dephosphorylates Cdk1-Y19 or inhibits a fourth phosphatase that does (Figure 2). In contrast, we have shown that PP2A^{Cdc55} does not regulate Cdk1-Y19 dephosphorylation independently of its function inhibiting Swe1 and activating Mih1 and cannot dephosphorylate Cdk1-Y19 *in vitro*. Acute loss of Cdc55 using an auxin-inducible degron, in fact, appears to cause more rapid dephosphorylation of Cdk1-Y19, suggesting that PP2A^{Cdc55} may negatively regulate Cdk1-Y19 dephosphorylation (Figure 2A). This function of PP2A^{Cdc55} may work via PP2A^{Rts1} because deletion of *RTS1* is epistatic to this behavior of *CDC55-AID*.

Although we have demonstrated that purified Mih1 and Ptp1 dephosphorylate Cdk1-Y19 *in vitro* (Figure 3), we were unable to rigorously test PP2A^{Rts1} function *in vitro*. PP2A^{Rts1} substrates are thought to be phosphorylated only on serine and threonine residues (Janssens and Goris 2001; Shi 2009), but past work has shown that PP2A can acquire activity against tyrosine residues *in vitro* in specific reaction conditions or in the presence of PTPA (encoded by Rrd1 and Rrd2 in budding yeast), whose *in vivo* role is poorly understood (Cayla *et al.* 1990; Van Hoof *et al.* 1994; Van Hoof 2001).

We found it surprising that *mih1*Δ *ptp1*Δ cells initiate anaphase and enter G_1 with little change in the level of Cdk1-Y19 phosphorylation. Our measurements of Cdk1-Y19 phosphorylation and Cdk1 activity in these cells suggest that an additional one-third of the active Cdk1/Clb2 complexes are inhibited in these cells compared to wild-type cells, which increases to half when cells are arrested by overexpression of Swe1 or activation of a *SWE1*-dependent checkpoint (Figure 1D). This difference suggests that there is sufficient Cdk1 activity in *mih1*Δ *ptp1*Δ cells to drive entry into mitosis and the metaphase-to-anaphase transition and that the difference between cell-cycle arrest and progression may reflect a small change in the extent of inhibition of Cdk1 or the targeted inhibition of a pool of Cdk1. Our data lead to the hypothesis that PP2A^{Rts1} acts with Mih1 and Ptp1 to activate this pool of Cdk1 activity.

One aim of this study was to assess whether preventing Cdk1-Y19 dephosphorylation would block anaphase onset in a similar way as we have described in cells overexpressing Swe1 or arrested by latA treatment (Lianga *et al.* 2013). Although *mih1*Δ *ptp1*Δ cells block Cdk1-Y19 dephosphorylation during anaphase in an unperturbed cell cycle (Figure 1B) and *mih1*Δ *ptp1*Δ *rts1*Δ cells block dephosphorylation in the *in vivo* phosphatase assay (Figure 2), both mutant combinations do not block anaphase onset, as judged by activation of the anaphase-promoting complex (APC) and loss of the cohesin subunit Mcd1 (Figure S2). These results may indicate that Cdk1-Y19 dephosphorylation is not needed to trigger anaphase, but we think that it is more likely that Cdk1-Y19 phosphorylation does not reach the level needed for cell-cycle arrest in these experiments. *rts1*Δ cells, like *CDC55-AID* cells, induce *GAL-SWE1-AID* poorly, and lower levels of Cdk1-Y19 phosphorylation accumulate in these cells prior to the addition of auxin and dextrose (Figure 2).

Numerous studies have suggested that inhibitory phosphorylation regulates Cdk1 activation in a stepwise manner in both vertebrates and yeast (Stern and Nurse 1996; Pomerening *et al.* 2003, 2005; Deibler and Kirschner 2010; Harvey *et al.* 2011). Lower levels of Cdk1 activity are needed to induce the entry into mitosis than the metaphase-to-anaphase transition, and Cdk1-Y19 phosphorylation functions at both these thresholds (Rahal and Amon 2008; Lianga *et al.* 2013). Our results suggest that at least three phosphatases regulate Cdk1 dephosphorylation and that the regulation of their activity may provide a mechanism for cells to activate pools of Cdk1 at different times and in different cellular locations. $PP2A^{Rts1}$ is localized to the pericentromere (Gentry and Hallberg 2002; Kitajima *et al.* 2006; Riedel *et al.* 2006), and its activity there may allow kinetochore activation of Cdk1 and assist in triggering anaphase onset.

Cdc25 inhibitors have been pursued as promising chemotherapeutic agents that could block cell-cycle progression in cancerous cells, but these compounds have had only limited clinical success (Lavecchia *et al.* 2012). If similar redundancy exists in human cells as we have uncovered in budding yeast, then several different phosphatase inhibitors may be needed to effectively block Cdk1 activation and arrest the cell cycle.

Acknowledgments

We thank Thomas Eng and Doug Koshland for plasmids; Doug Kellogg, Mark Hall, Kathy Gould, Mike Downey, Hilary Phenix, Dara Spatz Friedman, and current and former members of the Rudner laboratory for invaluable discussions, technical advice, and unwavering support. Immunization of rabbits for antibody production was performed at the Ottawa University Animal Care Facility. This work was supported by grants from the Canadian Institutes of Health Research (177774), the Canada Foundation for Innovation (13119), and the University of Ottawa Research Development Program–Bridge Funding Opportunity and CIHR New Investigator and Ontario Early Researcher awards. E.K.K. was supported by an Ontario Graduate Scholarship; M.D. was supported by a Natural Sciences and Engineering Research Council Undergraduate Student Research Award; and N.L. and E.C.W. were supported by CIHR Canada Graduate Fellowships.

Literature Cited

Booher, R. N., R. J. Deshaies, and M. W. Kirschner, 1993 Properties of Saccharomyces cerevisiae wee1 and its differential regulation of p34CDC28 in response to G_1 and G_2 cyclins. EMBO J. 12: 3417–3426.

Cayla, X., J. Goris, J. Hermann, P. Hendrix, R. Ozon *et al.*, 1990 Isolation and characterization of a tyrosyl phosphatase activator from rabbit skeletal muscle and Xenopus laevis oocytes. Biochemistry 29: 658–667.

Costanzo, M., A. Baryshnikova, J. Bellay, Y. Kim, E. D. Spear *et al.*, 2010 The genetic landscape of a cell. Science 327: 425–431.

Deibler, R. W., and M. W. Kirschner, 2010 Quantitative reconstitution of mitotic CDK1 activation in somatic cell extracts. Mol. Cell 37: 753–767.

Dunphy, W. G., and A. Kumagai, 1991 The cdc25 protein contains an intrinsic phosphatase activity. Cell 67: 189–196.

Foulkes, J. G., E. Erikson, and R. L. Erikson, 1983 Separation of multiple phosphotyrosyl- and phosphoseryl-protein phosphatases from chicken brain. J. Biol. Chem. 258: 431–438.

Gannon, J. V., A. Nebreda, N. M. Goodger, P. R. Morgan, and T. Hunt, 1998 A measure of the mitotic index: studies of the abundance and half-life of p34cdc2 in cultured cells and normal and neoplastic tissues. Genes Cells 3: 17–27.

Gautier, J., M. J. Solomon, R. N. Booher, J. F. Bazan, and M. W. Kirschner, 1991 cdc25 is a specific tyrosine phosphatase that directly activates p34cdc2. Cell 67: 197–211.

Gentry, M. S., and R. L. Hallberg, 2002 Localization of Saccharomyces cerevisiae protein phosphatase 2A subunits throughout mitotic cell cycle. Mol. Biol. Cell 13: 3477–3492.

Gould, K. L., and P. Nurse, 1989 Tyrosine phosphorylation of the fission yeast cdc2+ protein kinase regulates entry into mitosis. Nature 342: 39–45.

Gould, K. L., S. Moreno, N. K. Tonks, and P. Nurse, 1990 Complementation of the mitotic activator, p80cdc25, by a human protein-tyrosine phosphatase. Science 250: 1573–1576.

Hannig, G., S. Ottilie, A. R. Schievella, and R. L. Erikson, 1993 Comparison of the biochemical and biological functions of tyrosine phosphatases from fission yeast, budding yeast and animal cells. Yeast 9: 1039–1052.

Harvey, S. L., and D. R. Kellogg, 2003 Conservation of mechanisms controlling entry into mitosis: budding yeast wee1 delays entry into mitosis and is required for cell size control. Curr. Biol. 13: 264–275.

Harvey, S. L., A. Charlet, W. Haas, S. P. Gygi, and D. R. Kellogg, 2005 Cdk1-dependent regulation of the mitotic inhibitor Wee1. Cell 122: 407–420.

Harvey, S. L., G. Enciso, N. Dephoure, S. P. Gygi, J. Gunawardena *et al.*, 2011 A phosphatase threshold sets the level of Cdk1 activity in early mitosis in budding yeast. Mol. Biol. Cell 22: 3595–3608.

Healy, A. M., S. Zolnierowicz, A. E. Stapleton, M. Goebl, A. A. DePaoli-Roach *et al.*, 1991 CDC55, a Saccharomyces cerevisiae gene involved in cellular morphogenesis: identification, characterization, and homology to the B subunit of mammalian type 2A protein phosphatase. Mol. Cell. Biol. 11: 5767–5780.

Janssens, V., and J. Goris, 2001 Protein phosphatase 2A: a highly regulated family of serine/threonine phosphatases implicated in cell growth and signalling. Biochem. J. 353: 417–439.

Kellogg, D. R., 2003 Wee1-dependent mechanisms required for coordination of cell growth and cell division. J. Cell Sci. 116: 4883–4890.

Kitajima, T. S., T. Sakuno, K.-I. Ishiguro, S.-I. Iemura, T. Natsume *et al.*, 2006 Shugoshin collaborates with protein phosphatase 2A to protect cohesin. Nature 441: 46–52.

Lavecchia, A., C. Di Giovanni, and E. Novellino, 2012 CDC25 phosphatase inhibitors: an update. Mini Rev. Med. Chem. 12: 62–73.

Lew, D. J., and S. I. Reed, 1995 A cell cycle checkpoint monitors cell morphogenesis in budding yeast. J. Cell Biol. 129: 739–749.

Lianga, N., E. C. Williams, E. K. Kennedy, C. Doré, S. Pilon *et al.*, 2013 A Wee1 checkpoint inhibits anaphase onset. J. Cell Biol. 201: 843–862.

Millar, J. B., G. Lenaers, and P. Russell, 1992 Pyp3 PTPase acts as a mitotic inducer in fission yeast. EMBO J. 11: 4933–4941.

Minshull, J., A. Straight, A. D. Rudner, A. F. Dernburg, A. Belmont *et al.*, 1996 Protein phosphatase 2A regulates MPF activity and

sister chromatid cohesion in budding yeast. Curr. Biol. 6: 1609–1620.
Nurse, P., 1975 Genetic control of cell size at cell division in yeast. Nature 256: 547–551.
Nurse, P., 1990 Universal control mechanism regulating onset of M-phase. Nature 344: 503–508.
Pal, G., M. T. Z. Paraz, and D. R. Kellogg, 2008 Regulation of Mih1/Cdc25 by protein phosphatase 2A and casein kinase 1. J. Cell Biol. 180: 931–945.
Parker, L. L., S. Atherton-Fessler, and H. Piwnica-Worms, 1992 p107wee1 is a dual-specificity kinase that phosphorylates p34cdc2 on tyrosine 15. Proc. Natl. Acad. Sci. USA 89: 2917–2921.
Pomerening, J. R., E. D. Sontag, and J. E. Ferrell, 2003 Building a cell cycle oscillator: hysteresis and bistability in the activation of Cdc2. Nat. Cell Biol. 5: 346–351.
Pomerening, J. R., S. Y. Kim, and J. E. Ferrell, 2005 Systems-level dissection of the cell-cycle oscillator: bypassing positive feedback produces damped oscillations. Cell 122: 565–578.
Rahal, R., and A. Amon, 2008 Mitotic CDKs control the metaphase-anaphase transition and trigger spindle elongation. Genes Dev. 22: 1534–1548.
Riedel, C. G., V. L. Katis, Y. Katou, S. Mori, T. Itoh *et al.*, 2006 Protein phosphatase 2A protects centromeric sister chromatid cohesion during meiosis I. Nature 441: 53–61.
Rudner, A. D., K. G. Hardwick, and A. W. Murray, 2000 Cdc28 activates exit from mitosis in budding yeast. J. Cell Biol. 149: 1361–1376.
Russell, P., and P. Nurse, 1986 cdc25+ functions as an inducer in the mitotic control of fission yeast. Cell 45: 145–153.
Russell, P., and P. Nurse, 1987 Negative regulation of mitosis by wee1+, a gene encoding a protein kinase homolog. Cell 49: 559–567.
Russell, P., S. Moreno, and S. I. Reed, 1989 Conservation of mitotic controls in fission and budding yeasts. Cell 57: 295–303.
Shi, Y., 2009 Serine/threonine phosphatases: mechanism through structure. Cell 139: 468–484.
Shu, Y., H. Yang, E. Hallberg, and R. Hallberg, 1997 Molecular genetic analysis of Rts1p, a B′ regulatory subunit of Saccharomyces cerevisiae protein phosphatase 2A. Mol. Cell. Biol. 17: 3242–3253.
Stark, M. J., 1996 Yeast protein serine/threonine phosphatases: multiple roles and diverse regulation. Yeast 12: 1647–1675.
Stern, B., and P. Nurse, 1996 A quantitative model for the cdc2 control of S phase and mitosis in fission yeast. Trends Genet. 12: 345–350.
Tonks, N. K., 2013 Protein tyrosine phosphatases—from housekeeping enzymes to master regulators of signal transduction. FEBS J. 280: 346–378.
Van Hoof, C., 2001 The Saccharomyces cerevisiae phosphotyrosyl phosphatase activator proteins are required for a subset of the functions disrupted by protein phosphatase 2A mutations. Exp. Cell Res. 264: 372–387.
Van Hoof, C., X. Cayla, M. Bosch, W. Merlevede, and J. Goris, 1994 The phosphotyrosyl phosphatase activator of protein phosphatase 2A: a novel purification method, immunological and enzymic characterization. Eur. J. Biochem. 226: 899–907.
Welch, P. J., and J. Y. Wang, 1992 Coordinated synthesis and degradation of cdc2 in the mammalian cell cycle. Proc. Natl. Acad. Sci. USA 89: 3093–3097.
Zapata, J., N. Dephoure, T. Macdonough, Y. Yu, E. J. Parnell *et al.*, 2014 PP2ARts1 is a master regulator of pathways that control cell size. J. Cell Biol. 204: 359–376.
Zhao, Y., G. Boguslawski, R. S. Zitomer, and A. A. DePaoli-Roach, 1997 Saccharomyces cerevisiae homologs of mammalian B and B' subunits of protein phosphatase 2A direct the enzyme to distinct cellular functions. J. Biol. Chem. 272: 8256–8262.

Communicating editor: S. Biggins

GENETICS

Supporting Information
www.genetics.org/lookup/suppl/doi:10.1534/genetics.115.182469/-/DC1

Redundant Regulation of Cdk1 Tyrosine Dephosphorylation in *Saccharomyces cerevisiae*

Erin K. Kennedy, Michael Dysart, Noel Lianga, Elizabeth C. Williams, Sophie Pilon, Carole Doré, Jean-Sebastien Deneault, and Adam D. Rudner

DOI: 10.1534/genetics.115.182469

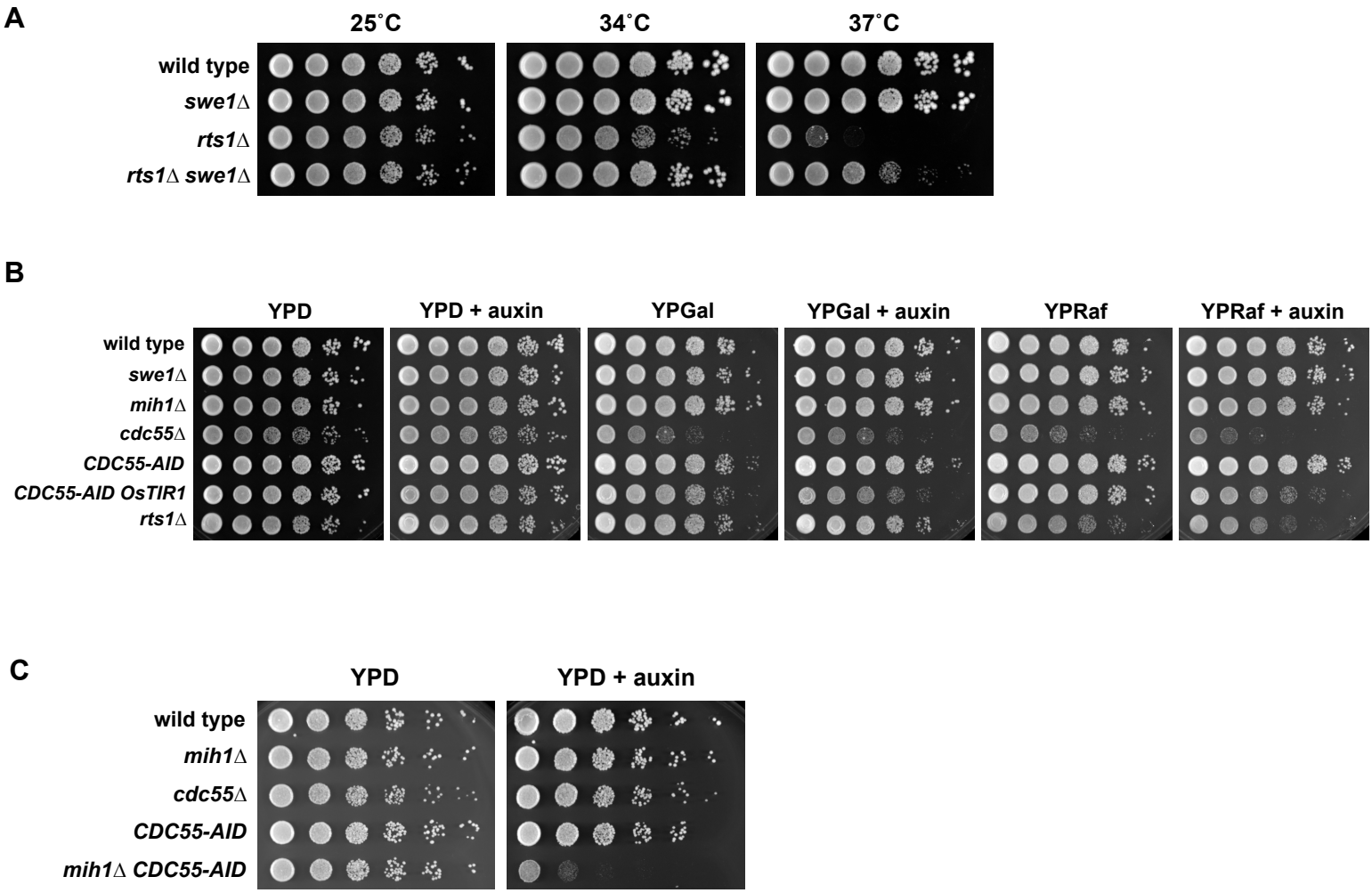

Figure S1. Additional analysis of *CDC55* and *RTS1.* (A) *rts1*Δ temperature sensitivity is partially suppressed by *swe1*Δ. Ten-fold serial dilutions of wild type, *swe1*Δ, *rts1*Δ and *rts1*Δ *swe1*Δ cells were spotted onto YPD plates and incubated at the indicated temperatures. **(B)** *cdc55*Δ and *CDC55-AID* grow poorly on non-fermentable carbon sources. Ten-fold serial dilutions of the indicated strains were spotted onto the indicated plates and incubated at 25˚C for two to three days. *cdc55*Δ grows poorly on YEP + 2% galactose (YPGal) and YEP + 2% raffinose (YPRaf) plates, and *CDC55-AID* cells, that also express *OsTIR1,* grow poorly on YPGal and YPRaf plates that contain 0.75mM auxin. **(C)** *mih1*Δ *CDC55-AID* cells are inviable on media containing auxin. Ten-fold serial dilutions of the indicated strains were spotted onto the indicated plates and incubated at 25˚C for two days.

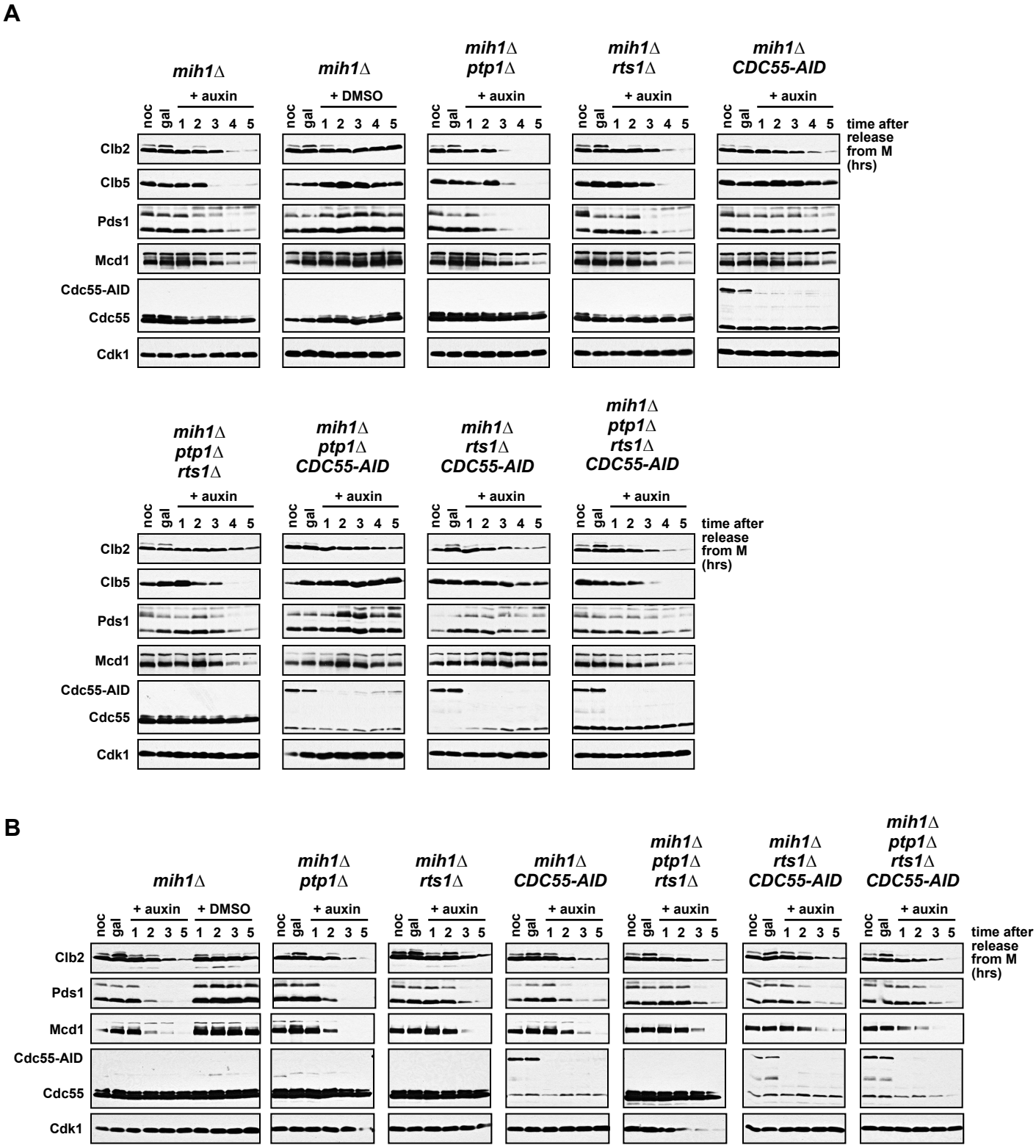

Figure S2. *mih1*Δ *ptp1*Δ *rts1*Δ cells do not arrest the cell cycle in the *in vivo* phosphatase assay. (A) Samples from Fig. 2A were immunoblotted with the indicated antibodies. When 25ng/ml α-factor is added to the cultures after release from the nocodazole arrest, *CDC55-AID* strains arrest the cell cycle as determined by the stability of APC substrates (Clb2, Clb5 and Pds1) and degradation of full length Mcd1. **(B)** Samples from Fig. 2B (as well as additional samples from three strains) were immunoblotted with the indicated antibodies. When 1μg/ml α-factor is added to the cultures after release from the nocodazole arrest, all strains treated with auxin do not arrest the cell cycle.

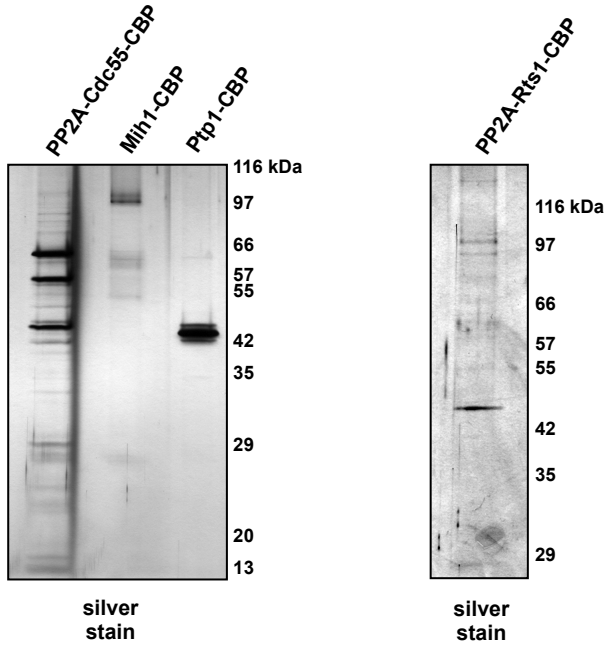

Figure S3. Purified phosphatases. Mih1-CBP and Ptp1-CBP were purified from cells harbouring *pGAL-MIH1-TAP-2μ* or *pGAL-PTP1-TAP-2μ* plasmids using a two-step TAP purification. PP2A-Cdc55 and PP2A-Rts1 complexes were purified from cells which contain an endogenously tagged *CDC55-TAP* or *RTS1-TAP.* 10% of each purification was separated by SDS-PAGE and silver stained.

Table S1 - Complete list of strains

Strain	Genotype[a]
ADR21	***MATa*** *ura3-1 leu2-3,112 trp1-1 his3-11,15 ade2-1 can1-100*
ADR22	***MATα*** *ura3-1 leu2-3,112 trp1-1 his3-11,15 ade2-1 can1-100*
ADR601	***MATa*** *swe1Δ::TRP1*
ADR2562	***MATa*** *pGAL-SWE1-HA-LEU2, bar1Δ*
ADR3173	***MATa*** *swe1Δ::TRP1 bar1Δ*
ADR4006	***MATa*** *bar1Δ*
ADR4031	***MATa*** *swe1Δ::LEU2-pGAL-SWE1-HA mih1Δ::kanMX bar1Δ*
ADR4215	***MATa*** *rts1Δ::kanMX*
ADR4217	***MATα*** *kanMX-CDC28-Y19F*
ADR5297	***MATa*** *RTS1-TAP-KITRP1 bar1Δ*
ADR5465	***MATa*** *CDC55-TAP-KITRP1 bar1Δ*
ADR6320	***MATa*** *CDC55-AID-kanMX bar1Δ*
ADR6385	***MATa*** *CDC55-AID-kanMX leu2::pGPD1-OsTIR1-LEU2 bar1Δ*
ADR6876	***MATa*** *cdc55Δ::hphMX bar1Δ*
ADR6929	***MATa*** *rts1Δ::hphMX*
ADR7368	***MATa*** *mih1Δ::hphMX CDC55-AID-kanMX leu2::pGPD1-OsTIR1-LEU2 bar1Δ*
ADR7447	***MATa*** *mih1Δ::hphMX leu2::pGPD1-OsTIR1-LEU2 bar1Δ*
ADR7921	***MATa*** *mih1Δ::hphMX CDC55-AID-kanMX swe1Δ::LEU2-pGAL-SWE1-AID-natMX trp1::pGPD1-OsTIR1-TRP1 SPC42-GFP-Sphis5⁺ bar1Δ*
ADR7942	***MATa*** *mih1Δ::hphMX ptp1Δ::CaURA3 bar1Δ*

ADR8041	***MATa*** *mih1Δ::kanMX CDC55-AID-kanMX swe1Δ::LEU2-pGAL-SWE1-AID-natMX trp1::pGPD1-OsTIR1-TRP1 SPC42-GFP-Sphis5⁺ bar1Δ*
ADR8300	***MATa*** *ptp1Δ::CaURA3*
ADR8304	***MATa*** *mih1Δ::kanMX ptp1Δ::CaURA3 rts1Δ::hphMX CDC55-AID-kanMX swe1Δ::LEU2-pGAL-SWE1-AID-natMX trp1::pGPD1-OsTIR1-TRP1 SPC42-GFP-Sphis5⁺ bar1Δ*
ADR9027	***MATα*** *rts1Δ::hphMX [RTS1-CEN-URA3 (pAR1286)]*
ADR9028	***MATa*** *[RTS1-CEN-URA3 (pAR1286)]*
ADR9029	***MATa*** *mih1Δ::LEU2 ptp1Δ::natMX [RTS1-CEN-URA3 (pAR1286)]*
ADR9030	***MATa*** *mih1Δ::LEU2 rts1Δ::hphMX [RTS1-CEN-URA3 (pAR1286)]*
ADR9031	***MATa*** *ptp1Δ::natMX rts1Δ::hphMX [RTS1-CEN-URA3 (pAR1286)]*
ADR9032	***MATa*** *mih1Δ::LEU2 ptp1Δ:: natMX rts1Δ::kanMX swe1Δ::TRP1 [RTS1-CEN-URA3 (pAR1286)]*
ADR9034	***MATa*** *mih1Δ::LEU2 ptp1Δ::natMX rts1Δ::hphMX [RTS1-CEN-URA3 (pAR1286)]*
ADR9422	***MATa*** *mih1Δ::kanMX ptp1Δ::CaURA3 swe1Δ::LEU2-pGAL-SWE1-AID-natMX trp1::pGPD1-OsTIR1-TRP1 SPC42-GFP-Sphis5⁺ bar1Δ::hphMX*
ADR9423	***MATa*** *mih1Δ::kanMX ptp1Δ::CaURA3 CDC55-AID-kanMX swe1Δ::LEU2-pGAL-SWE1-AID-natMX trp1::pGPD1-OsTIR1-TRP1 SPC42-GFP-Sphis5⁺ bar1Δ*
ADR9461	***MATa*** *ptp1Δ::CaURA3 bar1Δ*
ADR9475	***MATa*** *mih1Δ::kanMX rts1Δ::hphMX swe1Δ::LEU2-pGAL-SWE1-AID-natMX trp1::pGPD1-OsTIR1-TRP1 SPC42-GFP-Sphis5⁺ bar1Δ::CaURA3*
ADR9477	***MATa*** *mih1Δ::kanMX ptp1Δ::CaURA3 rts1Δ::hphMX swe1Δ::LEU2-pGAL-SWE1-AID-natMX trp1::pGPD1-OsTIR1-TRP1 SPC42-GFP-Sphis5⁺ bar1Δ::hphMX*
ADR9485	***MATa*** *mih1Δ::kanMX swe1Δ::LEU2-pGAL-SWE1-AID-natMX trp1::pGPD1-OsTIR1-TRP1 SPC42-GFP-Sphis5⁺ bar1Δ::hphMX*
ADR9532	***MATα*** *rts1Δ::kanMX swe1Δ::TRP1*

ADR9536	***MATα*** *rts1Δ::kanMX*
ADR9539	***MATα*** *swe1Δ::TRP1*

[a] All strains are isogenic to W303-1a (ADR21) and W303-1b (ADR22).

Table S2 - Strains used in each figure

Figure	Relevant genotype [a]	Strain number
1A	wild type	ADR4006
	*swe1*Δ	ADR3173
	*mih1*Δ	ADR7447
	*cdc55*Δ	ADR6876
	*rts1*Δ	ADR6929
	*ptp1*Δ	ADR8300
1B	wild type	ADR4006
	*mih1*Δ	ADR7747
	*ptp1*Δ	ADR9461
	*mih1*Δ *ptp1*Δ	ADR7942
1C	*mih1*Δ	ADR7747
	*mih1*Δ *ptp1*Δ	ADR7942
	wild type	ADR4006
	GAL-SWE1	ADR4031
1D	wild type	ADR4006
	*swe1*Δ	ADR3173
	*mih1*Δ	ADR7747
	*mih1*Δ *ptp1*Δ	ADR7942
	GAL-SWE1	ADR4031

1E	*[RTS1-CEN-URA3]*	ADR9028
	rts1Δ [RTS1-CEN-URA3]	ADR9027
	mih1Δ ptp1Δ [RTS1-CEN-URA3]	ADR9029
	mih1Δ rts1Δ [RTS1-CEN-URA3]	ADR9030
	ptp1Δ rts1Δ [RTS1-CEN-URA3]	ADR9031
	mih1Δ ptp1Δ rts1Δ [RTS1-CEN-URA3]	ADR9034
	mih1Δ ptp1Δ rts1Δ swe1Δ [RTS1-CEN-URA3]	ADR9032
2A	*mih1Δ pGAL-SWE1-AID*	ADR9485
	mih1Δ ptp1Δ pGAL-SWE1-AID	ADR9422
	mih1Δ rts1Δ pGAL-SWE1-AID	ADR9475
	mih1Δ CDC55-AID pGAL-SWE1-AID	ADR7921
	mih1Δ ptp1Δ rts1Δ pGAL-SWE1-AID	ADR9477
	mih1Δ ptp1Δ CDC55-AID pGAL-SWE1-AID	ADR9423
	mih1Δ rts1Δ CDC55-AID pGAL-SWE1-AID	ADR8041
	mih1Δ ptp1Δ rts1Δ CDC55-AID pGAL-SWE1-AID	ADR8304
2B	*mih1Δ GAL-SWE1-AID*	ADR9485
	mih1Δ ptp1Δ GAL-SWE1-AID	ADR9422
	mih1Δ rts1Δ GAL-SWE1-AID	ADR9475
	mih1Δ ptp1Δ rts1Δ GAL-SWE1-AID	ADR9477
3	*GAL-SWE1-HA*	ADR2562
	wild type	ADR4006
	CDC55-TAP	ADR5465

	RTS1-TAP	ADR5297
	*swe1*Δ	ADR601
	CDC28-Y19F	ADR4217
S1A	wild type	ADR22
	*swe1*Δ	ADR9539
	*rts1*Δ	ADR9536
	*rts1*Δ *swe1*Δ	ADR9532
S1B	Wild type	ADR4006
	*swe1*Δ	ADR601
	*mih1*Δ	ADR7747
	*cdc55*Δ	ADR6876
	CDC55-AID	ADR6320
	CDC55-AID OsTIR1	ADR6385
	*rts1*Δ	ADR4215
S1C	Wild type	ADR4006
	*mih1*Δ	ADR7747
	*cdc55*Δ	ADR6876
	CDC55-AID OsTIR1	ADR6385
	*mih1*Δ *CDC55-AID OsTIR1*	ADR7368
S2A	*mih1*Δ *GAL-SWE1-AID*	ADR9485
	*mih1*Δ *ptp1*Δ *GAL-SWE1-AID*	ADR9422

	mih1Δ rts1Δ GAL-SWE1-AID	ADR9475
	mih1Δ CDC55-AID GAL-SWE1-AID	ADR7921
	mih1Δ ptp1Δ rts1Δ GAL-SWE1-AID	ADR9477
	mih1Δ ptp1Δ CDC55-AID GAL-SWE1-AID	ADR9423
	mih1Δ rts1Δ CDC55-AID GAL-SWE1-AID	ADR8041
	mih1Δ ptp1Δ rts1Δ CDC55-AID GAL-SWE1-AID	ADR8304
S2B	*mih1Δ GAL-SWE1-AID*	ADR9485
	mih1Δ ptp1Δ GAL-SWE1-AID	ADR9422
	mih1Δ rts1Δ GAL-SWE1-AID	ADR9475
	mih1Δ CDC55-AID GAL-SWE1-AID	ADR7921
	mih1Δ ptp1Δ rts1Δ GAL-SWE1-AID	ADR9477
	mih1Δ rts1Δ CDC55-AID GAL-SWE1-AID	ADR8041
	mih1Δ ptp1Δ rts1Δ CDC55-AID GAL-SWE1-AID	ADR8304
S3	wild type	ADR4006
	swe1Δ	ADR601
	GAL-SWE1-HA	ADR2562
	CDC28-Y19F	ADR4217
	CDC55-TAP	ADR5465
	RTS1-TAP	ADR5297

[a] See Supplemental Table 1 for complete genotype

File S1. Methods

Strain and Plasmid Construction

Supplemental Table 1 lists the strains used in this work and Supplemental Table 2 lists the strains used in each figure. All strains are derivatives of the W303 strain background (W303-1a), see Table S1 for complete genotype. All deletions and replacements were confirmed by immunoblotting, phenotype or PCR. Strains were constructed by genetic cross and transformation. The sequences of all primers used in this study are available upon request. Phusion polymerase (NEB) was used for all PCR reactions. The bacterial strains TG1 and DH5α were used for amplification of DNA.

*cdc55*Δ::*hphMX, rts1*Δ*::hphMX, mih1*Δ*::hphMX* and *bar1*Δ*::hphMX* were constructed by amplifying *hphMX* off pAG32 (Goldstein and McCusker 1999) and deleting *CDC55, RTS1, MIH1* and *BAR1* respectively. *ptp1*Δ*::natMX* was constructed by amplifying *natMX* off pAG25 (Goldstein and McCusker 1999) and deleting *PTP1*. *mih1*Δ*::kanMX* and *rts1*Δ*::kanMX* was constructed by amplifying *kanMX* off pFA6a-kanMX6 (Longtine *et al.* 1998) and deleting *MIH1* and *RTS1*. *ptp1*Δ*::CaURA3* was constructed by amplifying *CaURA3* off pAR747 (Larin *et al.* 2015) and deleting *PTP1*. Unmarked *bar1*Δ was constructed using pJGsst1 (J. Thorner, University of California, Berkeley, CA). *mih1*Δ*::LEU2* was constructed using pIP33 (P. Sorger, Harvard Medical School, Boston, MA). *swe1*Δ*::TRP1* strains were made by crossing JM449 (J. Minshull, DNA2.0, Menlo Park, CA) to the appropriate strains.

RTS1-CEN-URA3 was constructed by PCR amplifying *RTS1* with upstream and downstream regions (207bp and 195bp, respectively) and cloning the PCR fragment into pRS316 digested with BamH1/Xho1 to create pAR1286.

swe1Δ::LEU2-pGAL-SWE1-HA was constructed using pSwe1-41 (a gift of Bob Booher, Onyx Pharmaceuticals, Richmond, CA; (Booher *et al*. 1993)). *swe1Δ::LEU2-pGAL-SWE1-AID-natMX* was constructed by amplifying *AID* and *natMX* off pAR1099 and integrating the resulting PCR product at *swe1Δ::LEU2-pGAL-SWE1-HA* to replace the HA tag with the AID tag. pAR1099 was created by cloning a Pac1/Sal1 *natMX* fragment from pAG25 into pAID1 (Nishimura *et al.* 2009) digested with Pac1/Sal1. *CDC55-AID-kanMX* was constructed by amplifying *AID* and *kanMX* off pAID1 and integrating the resulting PCR product at *CDC55*. *leu2::pGPD1-OsTIR1-LEU2* and *trp1::pGPD1-OsTIR1-TRP1* were constructed by digesting pTIR4 and pTIR6 (Nishimura *et al.* 2009) with Stu1 and Nde1, respectively, to integrate at *LEU2* or *TRP1* (plasmids were gifts of T. Eng and D. Koshland, UC, Berkeley, Berkeley, CA).

The *2μ-pGAL-CLB2-TAP-URA3* (pAR546), *2μ-pGAL-MIH1-TAP-URA3* (pAR1327) and *2μ-pGAL-PTP1-TAP-URA3* (pAR1328) were created by PCR amplifying *CLB2, MIH1* and *PTP1,* respectively, and the resultant PCR product, designed to have overlapping homology, was co-transformed into yeast along with pRS-AB1234 (C. Carroll and D.O. Morgan, UC San Francisco, San Francisco, CA) cut with BamH1 and HindIII. *CDC55-TAP-KlTRP1* and *RTS1-TAP-KlTRP1* strains were made using pBS1479 (Rigaut *et al.* 1999).

The construction of *kanMX-CDC28-Y19F* was described previously (Lianga *et al.* 2013).

Physiology

Unless noted in the figure legend, cells were grown in yeast extract peptone media + 2% dextrose (YEPD) at 25˚C or 30˚C. Cells cycle arrests were performed with 10μg/mL nocodazole (Sigma-Aldrich; made as a 10mg/ml stock in DMSO) and 1μg/mL α-factor (Biosynthesis; made

as a 10mg/ml stock in DMSO) for 3 hours. LatA was used at 2.5µM (Sigma-Aldrich or Tocris Biosciences). Auxin (indole-3-acetic acid, Sigma-Aldrich; made as a 1M stock in DMSO) was used at 500µM in liquid and solid media. Plate-based viability assays were performed using a multi-pronged serial dilution fork (DAN-KAR).

Western Blots

These methods have been described previously (Rudner *et al.* 2005; Lianga *et al.* 2013). Yeast extracts for Western blotting were made by bead beating (multitube bead beater; Biospec) frozen cell pellets in 1X sample buffer (2% SDS, 80mM Tris-HCl pH6.8, 10% glycerol, 10mM EDTA, bromophenol blue, 5% 2-mercaptoethanol). Samples were normalized by cell concentration before harvesting.

Standard methods were used for polyacrylamide gel electrophoresis and protein transfer to nitrocellulose (Pall). Typically, samples were run on 12.5% polyacrylamide gels (120:1 acrylamide:bis, respectively, with no added SDS). Blots were stained with Ponceau S to confirm transfer and equal loading of samples, and then were blocked for 30 min in blocking buffer (4% nonfat dried milk (Carnation) in TBST (20 mM Tris-HCl (pH 7.5), 150 mM NaCl, 0.1% Tween 20). All antibodies were incubated overnight at 4°C. Unless noted, primary antibodies were used in TBS-T with 4% fat free milk powder, 5% glycerol and 0.02 % NaN3. An autoclaved solution of 5% milk was used to make the 4% milk dilution buffer to increase the longevity of the antibody solution. After washing with TBST, the blots were incubated with horseradish peroxidase-conjugated anti-rabbit antibodies (Bio-Rad) at a 1:5,000 dilution in blocking buffer for 30 min at 25°C, washed again, incubated incubated in Western Lightning Plus-ECL (PerkinElmer). Signal detection was on HyBlot CL (Harvard Scientific) autoradiography film.

The use and production of 12CA5 ascites (BabCO), anti-Swe1, anti-Clb2, anti-Pds1, anti-Clb5, anti-Mcd1, anti-Cdk1, anti-Cdc2-Y15 (Cell Signaling) antibodies have been described previously (Kellogg and Murray 1995; Lianga *et al.* 2013). Anti-Cdc55 and anti-Rts1 rabbit polyclonal antibodies were used at 1:1000 and generated as follows: 1mg of GST-Cdc55 (aa322-462) and GST-Rts1 (aa1-150) was injected into rabbits every 4 weeks for 8 to 16 weeks (uOttawa animal facility). Rabbit serum was harvested, clarified by centrifugation and loaded on Affigel-10 (Bio-rad) columns coupled to purified malE-Cdc55 (aa322-462) and malE-Rts1 (aa1-150), respectively. Antibody was eluted from Affigel columns with either 100mM triethylamine pH 11.5 or 100mM glycine pH 2.3. The triethylamine and glycine elutions were neutralized, dialyzed in PBS + 50% glycerol and stored at -80°C.

GST-Cdc55 and GST-Rts1 were expressed from pAR739 and pAR740, respectively, in which Cdc55 (aa322-462) and Rts1 (aa1-150) were cloned as BamH1/EcoR1 fragments into pGEX-6P. malE-Cdc55 and malE-Rts1 were expressed from pAR1115 and pAR1116, respectively, in which Cdc55 (aa322-462) and Rts1 (aa1-150) were cloned as BamH1/Sal1 fragments into mMAL-c2 (NEB).

Immunoprecipitation and *in vitro* histone H1 kinase assays

These methods have been described previously (Rudner and Murray 2000). Cell pellets were lysed by mechanical disruption (Biospec mini beadbeater-16; 2 pulses of 20” with a 5’ incubation on ice between pulses) in APC lysis buffer (50 mM Hepes-KOH pH 7.8, 700 mM NaCl, 150 mM NaF, 150 mM Na-β-glycerophosphate pH 8.3, 1 mM EDTA, 1 mM EGTA, 5% glycerol, 0.25% NP-40, 1 mM DTT, 1 mM PMSF, 1 mM Na_3VO_4, 1 mM benzamidine, and leupeptin, bestatin, pepstatin A and chymostatin all at 1 mM), lysates clarified by centrifugation

(5’ at top speed in a microfuge) and Clb2 complexes isolated by immunoprecipitation using 0.5µl of anti-Clb2 antibody and proteinA coupled dynabeads (Invitrogen). Beads were washed three times in APC lysis buffer, split in half into fresh tubes during the third wash, and washed one time in kinase buffer (20mM Tris-HCl, pH 8.0, 50mM NaCl, 5mM $MgCl_2$, 0.01% NP-40, 1mM DTT). One set of beads was incubated in 15µl kinase buffer containing 2.5µg histone H1 (Upstate Biotechnology), 0.01 mM ATP and 1 µCi **γ-**[^{32}P]ATP for 20’ at 25˚C and the reaction was stopped by addition of 15µl 2X sample buffer. Reactions were analyzed by PAGE, dried and exposed to phosphorimager screen and the phosphorylation of histone H1 was quantified on a Typhoon Trio Phosphorimager and ImageQuant software (GE). Cdk1/Clb2 complexes were eluted from the other set of beads with 1X sample buffer, separated by PAGE, immunoblotted with anti-Cdk1 and anti-Cdc2-Y15 (Cell Signaling) antibodies, and the amount of Cdk1 and Cdk1-P-tyr in each IP was quantified using a ImageQuant LAS4000 imager and ImageQuant software (GE).

***In vivo* Cdk1-Y19 phosphatase assay**

Cultures were grown overnight at 25˚C in YEP + 2% raffinose and arrested in mitosis using nocodazole (Sigma-Aldrich) for 2.5 hrs at 25˚C. Galactose (2%) was then added while cultures were still arrested for 30 min. Cells were harvested, and washed in YPD + 500µM auxin (or DMSO vehicle) to release from the nocodazole arrest, to repress transcription from the *pGAL* promoter and activate Tir1/SCF-dependent degradation of AID-tagged proteins. α-factor was added at t=1 hr following release to capture cells in G1. Samples were taken every hour min for 5 hrs and analyzed by Western blot.

***In vitro* phosphatase assay**

GAL-SWE1-TAP (ADR2562) was grown overnight at 25˚C in YEP + 2% raffinose and induced with 2% galactose for 6 hrs. Cultures were harvested, washed with 50mM Hepes-KOH pH7.8, and 2 ml of APC lysis buffer was added per gram of pellet and lysed by bead beating (BioSpec) with acid washed glass beads (BioSpec). Lysate was clarified by centrifugation at 16,000X g for 10 min at 4˚C. 1µl of 12CA5 anti-HA (BabCO) was incubated with the lysate on ice for 10 min, 5µl of protein G-coupled magnetic beads (Invitrogen) was added per 100µl of lysate and incubated for 1 hr at 4˚C with rotation. Beads were washed 3X with APC lysis buffer and resuspended in Kinase buffer (20 mM HEPES pH 7.5 KOH, 5 mM MgCl2, 5% glycerol).

Cdk1/Clb2-CBP, Cdk1-F/Clb2-CBP, Mih1-CBP and Ptp1-CBP were purified from cells containing pAR546 (*2µ-pGAL-CLB2-TAP*), pAR1327 (*2µ-pGAL-MIH1-TAP*) and pAR1328 (*2µ-pGAL-PTP1-TAP)*, respectively, after induction by growth in galactose. Cdc55-CBP and Rts1-CBP complexes were purified from asynchronously growing *CDC55-TAP* (ADR5465) or *RTS1-TAP* (ADR5297) cells.

Protein complexes were purified as described previously (Rudner *et al.* 2005; Lianga *et al.* 2013). Harvested cells were lysed in APC lysis buffer by mechanical disruption with 0.5mm glass beads (Biospec mini beadbeater-16 for small scale purification (1-5 grams; 2 pulses of 20” with a 5’ incubation on ice between pulses), or Biospec blender beadbeater for large scale scale purification (5-20 grams; 10 pulses of 30” with 30” incubation in an ice bath)). Lysate was clarified by centrifugation (microfuge for 10’ or Sorval SA-600 rotor at 15,000 rpm for 20’), and incubated with

100-500µl of a slurry of IgG-sepharose (GE) for four hours. Beads were pelleted at 500g, washed one time in lysis buffer, and transferred into a 3 ml column (Bio-rad bio-spin disposable chromatography column), and washed extensively with lysis buffer and TEV cleavage buffer (10mM Tris-HCl pH 8.0, 150mM NaCl, 0.5mM EDTA, 5% glycerol, 0.1% NP-40, and added just before use 1mM DTT, 1mM PMSF). Beads were incubated overnight at 4˚C in an equal volume of TEV cleavage buffer and 10-20µl of TEV protease. After cleavage the column was drained and the supernatant was supplemented with 5mM $CaCl_2$ and 10mM 2-mercaptoethanol, mixed with 100µl of calmodulin-Sepharose in a new 3ml column and incubated for 1-2 hours at 4˚C. The resin was then washed extensively in CaM binding buffer (10mM Tris-HCl pH 8.0, 150mM NaCl, 0.5mM EDTA, 5% glycerol, 0.1% NP-40, 1mM $MgCl_2$, 2mM $CaCl_2$ and added just before use 10mM 2-mercaptoethanol, 1mM PMSF), and the protein complexes eluted in CaM elution buffer (CaM binding buffer in which the $CaCl_2$ is replaced with 10mM EGTA) either in batch or in 200µl fractions. Fractions were analyzed by gel electrophoresis followed by silver staining, and for Cdk1/Clb2-CBP complexes, tested by *in vitro* phosphorylation of histone H1 in the presence of γ-[^{32}P]-ATP.

Purified Cdk1/Clb2-CBP and Cdk1-F/Clb2-CBP complexes were incubated with purified Swe1 (on beads) in kinase buffer with 1 mM DTT, 0.001 mM ATP, 1µCi of γ-[^{32}P]-ATP (Perkin Elmer) for 60 min at room temperature. Beads were removed and the phosphorylated Cdk1 complexes were mixed with purified phosphatases or lambda phosphatase (NEB), and 1mM ATP. Lambda phosphatase was inhibited by removing $MnCl_2$ from the reaction. Reactions were incubated for 40 minutes at room temperature

and stopped by the addition of 2X sample buffer. Samples were analyzed by PAGE, dried and exposed to phosphorimager screen, and imaged using a Typhoon Trio Phosphorimager (GE).

References

Booher R. N., Deshaies R. J., Kirschner M. W., 1993 Properties of Saccharomyces cerevisiae wee1 and its differential regulation of p34CDC28 in response to G1 and G2 cyclins. EMBO J **12**: 3417–3426.

Goldstein A. L., McCusker J. H., 1999 Three new dominant drug resistance cassettes for gene disruption in Saccharomyces cerevisiae. Yeast **15**: 1541–1553.

Kellogg D. R., Murray A. W., 1995 NAP1 acts with Clb1 to perform mitotic functions and to suppress polar bud growth in budding yeast. **130**: 675–685.

Larin M. L., Harding K., Williams E. C., Lianga N., Doré C., Pilon S., Langis É., Yanofsky C., Rudner A. D., 2015 Competition between Heterochromatic Loci Allows the Abundance of the Silencing Protein, Sir4, to Regulate de novo Assembly of Heterochromatin. (HD Madhani, Ed.). PLoS Genet **11**: e1005425.

Lianga N., Williams E. C., Kennedy E. K., Doré C., Pilon S., Girard S. L., Deneault J.-S., Rudner A. D., 2013 A Wee1 checkpoint inhibits anaphase onset. **201**: 843–862.

Longtine M. S., McKenzie A., Demarini D. J., Shah N. G., Wach A., Brachat A., Philippsen P., Pringle J. R., 1998 Additional modules for versatile and economical PCR-based gene deletion and modification in Saccharomyces cerevisiae. Yeast **14**: 953–961.

Nishimura K., Fukagawa T., Takisawa H., Kakimoto T., Kanemaki M., 2009 An auxin-based degron system for the rapid depletion of proteins in nonplant cells. Nat. Methods **6**: 917– 922.

Rigaut G., Shevchenko A., Rutz B., Wilm M., Mann M., Séraphin B., 1999 A generic protein purification method for protein complex characterization and proteome exploration. Nat Biotechnol **17**: 1030–1032.

Rudner A. D., Murray A. W., 2000 Phosphorylation by Cdc28 activates the Cdc20-dependent activity of the anaphase-promoting complex. **149**: 1377–1390.

Rudner A. D., Hall B. E., Ellenberger T., Moazed D., 2005 A nonhistone protein-protein interaction required for assembly of the SIR complex and silent chromatin. Mol Cell Biol **25**: 4514–4528.